

# Determination of $J$ - $R$ curve of polypropylene copolymers using the normalization method

C. MORHAIN, J. I. VELASCO\*

Centre Català del Plàstic (CCP), Universitat Politècnica de Catalunya (UPC)  
C/Colom 114, E-08222 Terrassa (Barcelona), Spain

In this paper the applicability of the load normalization method to determine  $J$ - $R$  curves of polypropylene copolymers (PP) is analyzed. This method allows the determination of resistance curves ideally from a single fracture test, and it is based on the load separation principle, which assumes that load can be separated in two multiplicative functions, the geometry function,  $G(a/W)$ , and the deformation function,  $H(v_{pl}/W)$ , which depend of the crack depth and the plastic displacement, respectively. The load separation validity has been checked for two different PP copolymers (block and random copolymers) and the load normalization method has been applied in order to determine and analyze the resistance curves, which have been compared, as a reference, with those obtained by the multiple specimen method. The applicability of the load normalization method to PP copolymers is analyzed by introducing some variations in the general procedure: Firstly, the deformation function is determined using either a power law fit or the so-called LMN function. With the power law, two different fitting methods have been tested: the usual "6 + 1" method and a "6 + 6" method proposed here for giving more weight to the final point of the curve. Secondly, the influence of the material crack tip blunting has been analyzed quantifying it through different values of the constriction factor ( $m$ ) in the general expression of the blunting line. Finally, the effect of the separable blunting region extension on the  $J$ - $R$  curve has been also analyzed by establishing different separable blunting zones.

© 2001 Kluwer Academic Publishers

## 1. Introduction

The  $J$ -integral is one of the most utilised concept to characterise the fracture toughness of ductile polymeric materials, due to the high contribution of plastic deformation involved during the fracture of these materials. Generally, fracture behaviour is studied through the determination of the crack growth resistance curve ( $J$ - $R$  curve) where  $J$ -integral value is plotted as a function of the crack extension,  $\Delta a$ . The experimental determination of the  $J$ - $R$  curve requires a measurement of the crack extension during the test. The most utilised method for  $J$ - $R$  curve determination is the multiple-specimen method proposed by Begley and Landes [1] and normalised by ASTM [2] for metals and by ESIS [3] for polymeric materials. In this method, identical specimens are loaded monotonically to various values of loadline displacement in order to obtain different levels of crack extension and then fully unloaded. The specimens are then broken in brittle conditions and a direct measurement of crack extension can be realised on the fracture surface. Due to the high time and material consumption of this method, considerable attention has been paid to the development of alternative test methods that require a smaller number of specimens. The normalisation method proposed by

Landes and Herrera [4] allows the determination of the  $J$ - $R$  curve ideally through a single fracture test. In this method, the deformation properties are assumed to follow a reproducible curve in which load, displacement and crack length are uniquely related. Considering the work of Ernst *et al.* [5, 6] it can be assumed that load can be separated in two independent and multiplicative functions, which depend respectively to geometry and plastic displacement, and the key of the normalisation method lies thus in determining these functional relationships.

Since the relationship between load and geometry has been determined for several specimen geometries (SENB, CT, . . .) [7], the main interest of the normalisation method resides in determining the relationship between load and plastic displacement. For this, the method assumes a functional form with unknown constants for the calibration curve of normalised load versus plastic displacement, and determines the constants at known calibration points, namely where load, displacement and crack length are known simultaneously. Finally, as the functional relationship between load, displacement and crack length is completely defined, the crack length value can be determined at any instant of the test.

\* Author to whom all correspondence should be addressed.

Although normalisation method was firstly applied to metallic materials [4, 8–10], it has been also successfully applied to different kinds of polymeric materials, either glassy (ABS [11], rubber-modified PS [12], PVC [13], PC [14] and toughened amorphous nylon [15]), as crystalline (toughened PA66 [15], MDPE [16] and a thermally treated homopolymer PP [12]). The procedure of the method has suffered some modifications since its development by Landes and Herrera [4]. Several functional forms have been proposed to describe the deformation function. The original work [4] considered that a power law equation described adequately the deformation behaviour of the material. Although this functional form gave consistent results, a second form consisting in a combination of a power law and a straight line was proposed, based on the observation of many true stress versus true strain tensile curves [17]. Finally, it has been reported that the use of the LMN function developed by Orange [18] results in a better accuracy of the  $J$ - $R$  curve, especially for low increments of crack length [10]. Considering the calibration points used to determine the constants of the functional form, some corrections have been also introduced to take into account the variations of crack length in the initial stage of the test due to crack tip blunting [10].

Despite the fact that load separation has been analytically demonstrated for Ramberg-Osgood materials [19], it has been only experimentally checked for a few number of metallic [7–9] and polymeric [11, 12, 14, 16, 20] materials. The aim of the present work is to study the applicability of this method for determining the resistance curve of two different types of polypropylene materials (block and random copolymers). For the polymers studied in this work, the validity of the separation principle has been checked using the load separation criterion proposed by Sharobeam and Landes [7], and the geometry function has been experimentally determined. During the application of the normalisation method a special attention has been paid to the study of the influence of the functional form used for the calibration curve on the resulting  $J$ - $R$  curve. The influence of the way that crack tip blunting is introduced in the procedure has also been studied and the discussion of the results of the normalisation method is based on the comparison with the resistance curve obtained by the multiple specimen method.

## 2. Theoretical background

### 2.1. Load separation principle

The principle of load separation, firstly proposed by Rice [21], allows load,  $P$ , to be written as a function of the crack length,  $a$ , and plastic displacement,  $v_{pl}$ , by two separate multiplicative functions [5]:

$$P = G(a/W) \times H(v_{pl}/W) \quad (1)$$

$W$  is the specimen width,  $G$  and  $H$  are the so-called geometry and deformation functions. The plastic displacement is obtained from the total displacement,  $d$ , and the elastic displacement,  $v_{el}$ :

$$v_{pl} = d - v_{el} = d - C(a/W)P \quad (2)$$

where  $C(a/W)$  is the compliance.

The load separation criterion proposed by Sharobeam and Landes [7] introduces the separation parameter,  $S_{ij}$ , defined as the ratio between the load values obtained with two specimens with stationary crack length,  $a_i$  and  $a_j$ , at constant  $v_{pl}$ :

$$S_{ij} = \frac{P(a_i; v_{pl})}{P(a_j; v_{pl})} \Big|_{v_{pl}} \quad (3)$$

Combining Equations 1 and 3:

$$S_{ij} = \frac{G(a_i/W) \times H(v_{pl}/W)}{G(a_j/W) \times H(v_{pl}/W)} \Big|_{v_{pl}} = \frac{G(a_i/W)}{G(a_j/W)} \Big|_{v_{pl}} \quad (4)$$

The load separation criterion establish that load is separable for stationary cracks when the separation parameter  $S_{ij}$  maintains a constant value over the whole domain of plastic displacement.

The geometric factor ( $\eta_{pl}$ ) can be determined using the analytical form obtained by Sharobeam and Landes [7] from the derivation of the separable form:

$$\eta_{pl} = \frac{dG(b/W)/d(b/W)}{G(b/W)} \frac{b}{W} \quad (5)$$

where  $b$  is the ligament length ( $b = W - a$ ).

The geometry function can be determined from experimental data by using the separation parameter values obtained from different test records, as follows:

$$S_{ij} = C_1 G(b_i/W) \quad (6)$$

being ( $b_j/W$ ) constant.

The curve  $S_{ij}$  versus  $b_i/W$  gives the functional relationship between the geometry function and the ligament length, which is usually approximated by a power law fit:

$$G(b_i/W) = C_2 (b_i/W)^{C_3} \quad (7)$$

Thus, from Equations 5 and 7, it can be noted that  $\eta_{pl} = C_3$ .

### 2.2. Load normalization method

Once the geometry function is known, the normalized load can be obtained:

$$P_N = \frac{P}{G(a/W)} = H(v_{pl}/W) \quad (8)$$

The determination of the relationship between normalized load and normalized plastic displacement requires the emission of a hypothesis about its functional form. The functional form initially used by Landes and Herrera [4] followed a power law expression:

$$P_N = \beta (v_{pl}/W)^n \quad (9)$$

Although good results were obtained with this expression [11, 22, 23] it was observed that a better accuracy was obtained for the initial region (small crack growth)

of the  $J$ - $R$  curve when a combination of a power law and a straight line was used [14]. These results encouraged the utilization of the so-called LMN function, defined by Orange [18] as:

$$P_N = \frac{L + M(v_{pl}/W)}{N + (v_{pl}/W)} \left( \frac{v_{pl}}{W} \right) \quad (10)$$

This functional form has the advantage of describing a power law at low plastic displacement level and a straight line at high plastic displacement level, and its good convergence for metals [10] has been also confirmed for certain glassy polymers as PVC [13] and PC [14].

Once geometry and deformation functions are known, the instantaneous values of the crack length can be calculated by solving the next equation through a numerical routine:

$$P_N = \frac{P}{G(a/W)} = H \left( \frac{d - PC(a/W)}{W} \right) \quad (11)$$

The instantaneous values of  $d$  and  $P$  are known from the test and  $C(a/W)$  is the compliance. The resistance ( $J - \Delta a$ ) curve can then be easily determined with the calculated  $\Delta a$  and  $J$ -integral values. The  $J$ -integral approximate expression is used for this purpose:

$$J_0 = \frac{\eta U}{B(W - a_0)} \quad (12)$$

And corrected for crack growth [3]:

$$J = J_0 \left[ 1 - \frac{(0.75\eta - 1)\Delta a}{W - a_0} \right] \quad (13)$$

where  $U$  is the energy measured as the area under the load/displacement curve, and  $a_0$  is the initial crack length.

### 3. Experimental procedure

Two polypropylene injection grades were studied: PPB (Isplen PB140), a block copolymer produced by Repsol Química S.A. and PPR (Novolen 3200H), a random copolymer produced by Targor. The basic characteristics of these materials are shown in Table I.

Prismatic bars with nominal dimensions  $6.35 \times 12.7 \times 127 \text{ mm}^3$  were injection-molded using a Mateu-Solé 440/90 injection-molding machine. The

TABLE I Basic characteristics of the studied PP copolymers

Material	MFI <sup>(1)</sup> (g/10 min)	HDT <sup>(2)</sup> (°C)	Vicat <sup>(3)</sup> (°C)	% ethylene <sup>(4)</sup>	$\sigma_y^{(5)}$ (MPa)
PPB	3.5	55	70	10-11	20.1
PPR	2.4	50	65	2-3	25.1

<sup>(1)</sup> Measured at 230°C, with 2160 g.

<sup>(2)</sup> Measured at 120°C/h with 1.8 MPa.

<sup>(3)</sup> Measured at 120°C/h with 50 N.

<sup>(4)</sup> From manufacturer data.

<sup>(5)</sup> Tensile yield stress determined at room temperature and at 1 mm/min.

nominal injection pressure was 100 MPa and the barrel maximum temperature 190 °C. All the specimens were annealed at 110 °C during 24 h in order to release residual stresses. Any deformed specimen was rejected.

Three point bending tests were performed on single edge notched bend (SENB) specimens (span  $S = 50.8 \text{ mm}$ ) at a crosshead speed of 1 mm/min using a universal testing machine (Instron 4507). The specimens were obtained by cutting the injected prismatic bars into halves. The nominal dimensions of the specimens were  $B \times W \times L = 6.35 \times 12.7 \times 63.5 \text{ mm}^3$ , and the true dimensions had to be measured in each specimen due to the high degree of cooling shrinkage of polypropylene. A notch was inserted centrally in the narrowest side of each specimen, using a 45° V notch broaching tool with a notch tip radius of 0.25 mm. Two kind of tests were realized: On one side, three-point bend tests were performed on these blunt notched specimens in order to retard crack initiation up to sufficiently large displacements and, thus, apply the load separation criterion. Notch depth to width ratios of  $0.48 < a_0/W < 0.73$  were used.

On the other side, fracture tests were carried out on precracked specimens in order to apply the normalization method. These specimens were obtained by sharpening the blunt notches (typical deep of the sharpened zone 200  $\mu\text{m}$ ) with a single cut from a razor blade (approximate tip radius 0.1–0.2  $\mu\text{m}$ ). According to the ESIS protocol for plastic materials [3] the crack deep was always in the range  $0.55 < a_0/W < 0.65$ . The final crack length was measured directly on the fracture surface, after completing the specimen fracture in brittle conditions.

## 4. Results

### 4.1. Analysis of load separation validity

Initially, load/displacement curves were obtained by testing blunt notched specimens having different  $b/W$  ratio. These plots and the corresponding load/plastic displacement curves are shown in Figs 1 and 2, respectively. Since at low displacement levels the influence of notch tip blunting is negligible, the compliance,  $C(a/W)$ , could be taken as a constant value in the plastic displacement calculation.

According to Equation 3, the separation parameter  $S_{ij}$  was determined for seven specimens with different ligament length, and its evolution relative to the plastic displacement has been plotted in Fig. 3.

In this figure, leaving aside the irregularities provoked by oscillations of the load recorded in the test, one can see that the separation parameter maintains a constant value over the plastic displacement, except in a short region limited to the early plastic deformation ( $v_{pl} < v_{plmin}$ ). This initial variation of  $S_{ij}$  has been observed in both metallic [7, 8] and plastic [12, 14, 20] materials, and it is usually associated to the transition from the elastic to the plastic behavior. Thus, from the observed mean constancy of  $S_{ij}$  load separation is assumed for both kinds of polypropylene studied here, except for very low values of plastic displacement. Also, it can be observed that beyond a certain value of

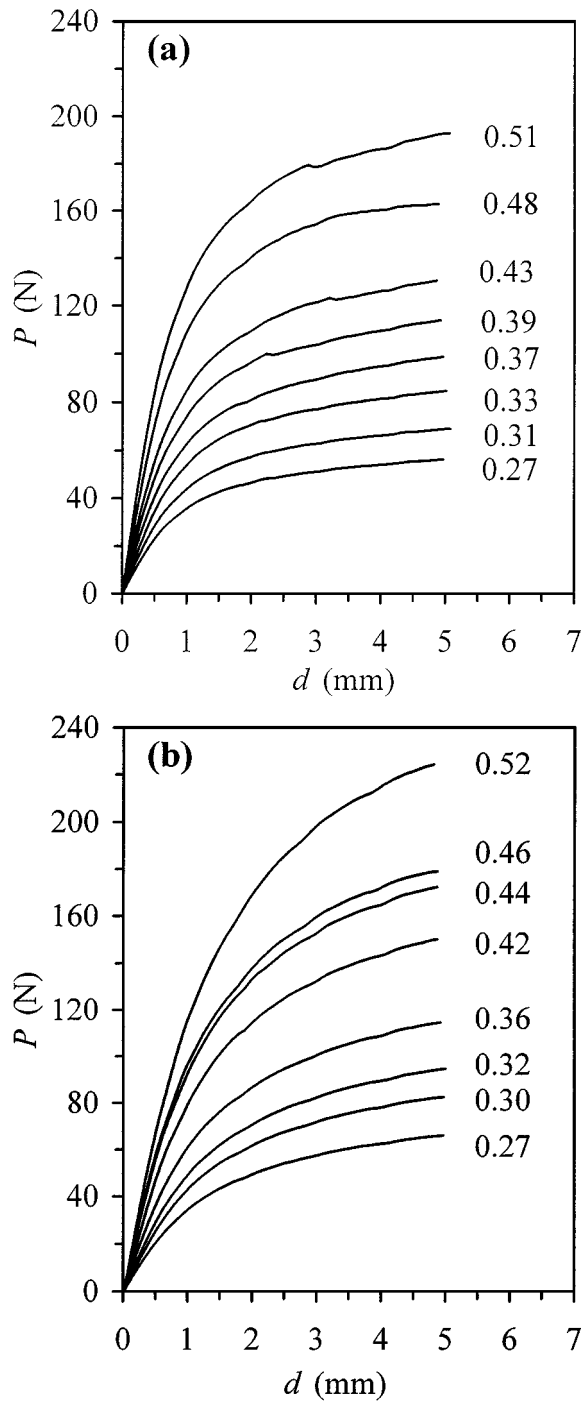


Figure 1 Load/displacement records for (a) PPB and (b) PPR. Numbers indicate the ligament length to width ratio.

plastic displacement the separation parameter tends to decrease slightly in specimens with higher ligament length. This slight decrease seems to be promoted by the notch tip blunting behavior, since the higher the specimen ligament length, the higher the energy stored by the specimen at a constant value of displacement in the test, and thus the higher the increment of notch length due to the tip blunting.

Once load separation is assumed, the geometry function,  $G(b/W)$ , could be determined from the relationship between  $S_{ij}$  and  $b_i$ . Values of  $S_{ij}$  against  $b_i/W$  have been plotted in Fig. 4 for both kinds of PP copolymers, and fitted according to a power law. In Table II the resulting values of  $\eta_{pl}$  for different plastic displacements have been compiled, and the average value ( $\eta_{pl}^{av}$ )

TABLE II  $\eta_{pl}$  values obtained by graphical determination

Plastic displacement (mm)	$\eta_{pl}(PPB)$	$\eta_{pl}(PPR)$
0.5	2.05	1.83
1	2.05	1.84
1.5	2.07	1.84
2	2.06	1.82
2.5	2.04	1.82
3	2.02	1.80
$\eta_{pl}^{av}$ ( $0.5 < v_{pl} < 2$ mm)	2.05	1.83

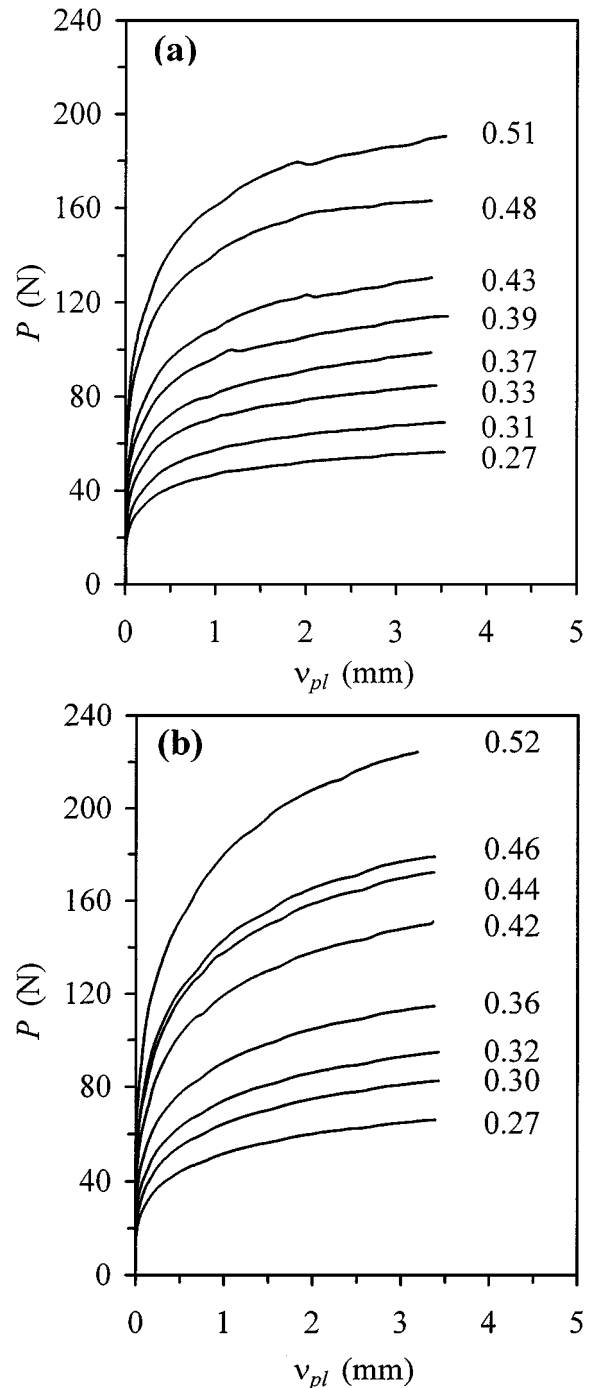


Figure 2 Load/plastic displacement curves for (a) PPB and (b) PPR. Numbers indicate the ligament length to width ratio.

is also shown; for specimens with larger ligament length only the region of plastic displacement where  $S_{ij}$  remained constant was considered in the average.

A proof of the analysis goodness is the low dispersion level of the  $\eta_{pl}$  values found, with the exception

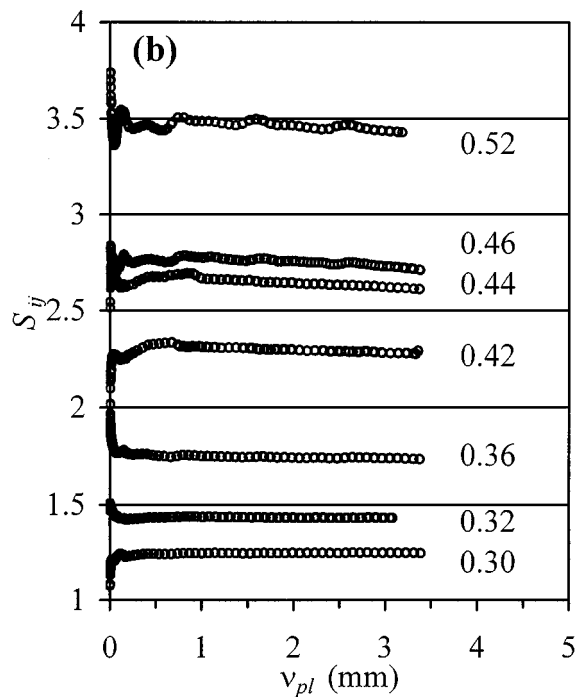
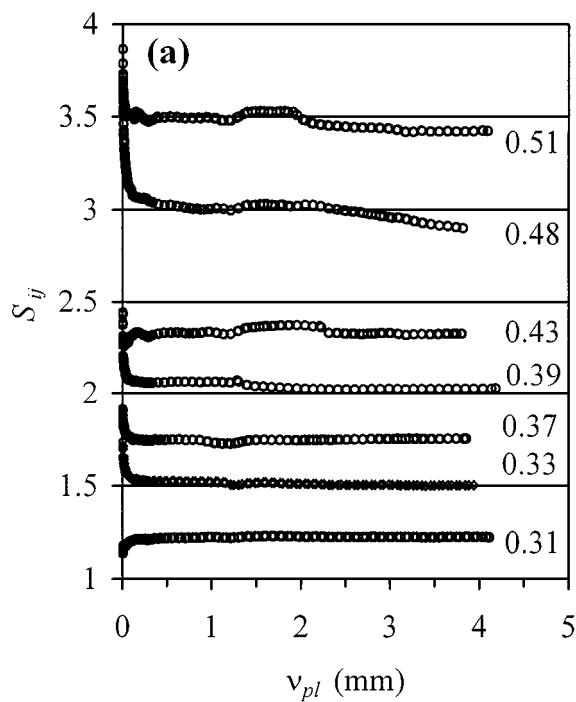


Figure 3 Evolution of the separation parameter  $S_{ij}$  with plastic displacement for (a) PPB and (b) PPR. Numbers indicate the  $b_j/W$  value.

of values from higher plastic displacement, which seems to be due to the negative influence of specimens with larger ligament length. The  $\eta_{pl}$  values found for polypropylene block copolymer are very close to the theoretical value for SENB geometry ( $\eta_{pl} = 2$ ) [24], while for polypropylene random copolymer the differences between the theoretical and the obtained values results higher. In this sense, values of  $\eta_{pl} \neq 2$  have been experimentally found by Frontini *et al.* [12] for a thermally treated PP homopolymer, being  $\eta_{pl}$  comprised between 1.9 and 2.2. Although these differences could be due to experimental error, Sharobeam and Landes [7] indicate that values of  $\eta_{pl} < 2$  may point out the dependence of  $\eta_{pl}$  on the material work hardening exponent with the convergence of their values to the analytically obtained values for very high work hardening

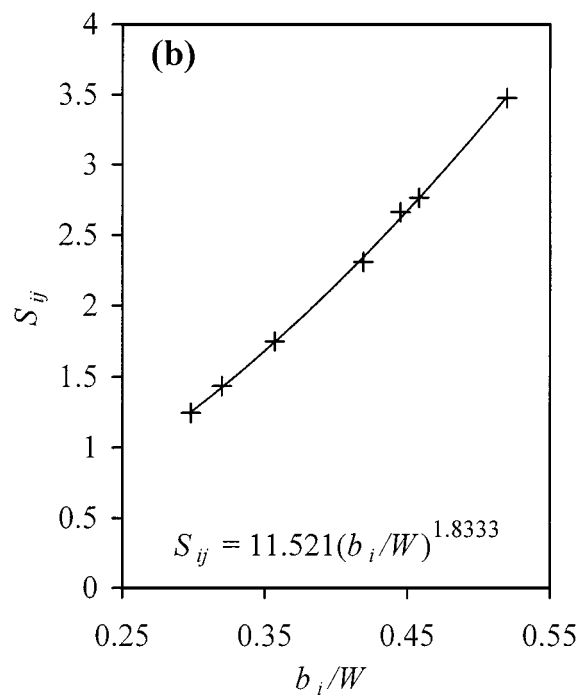
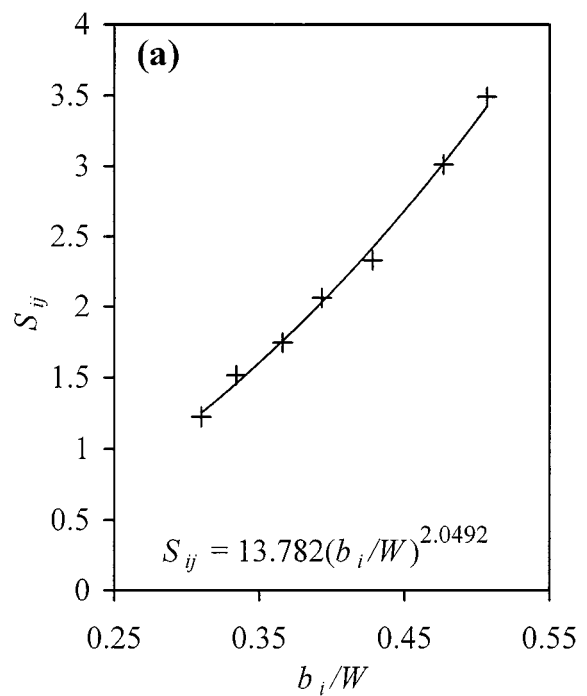


Figure 4 Determination of the relationship between the separation parameter and the remaining ligament, for (a) PPB and (b) PPR.

exponent values. In this sense, when fitting stress/strain data of PPB and PPR to the Ramberg-Osgood equation [25] we obtained (Fig. 5) a higher value of the work hardening exponent for PPR than for PPB, which does not support the observation of Sharobeam and Landes.

For the application of the load normalization method, which is shown in the following sections of this paper, the generally accepted expression of  $G(b/W)$  for SENB geometry [6] was employed for both copolymers:

$$G(b/W) = BW(b/W)^2 \quad (14)$$

That is, the theoretical value of  $\eta_{pl}$  was taken equal to 2 in both cases.

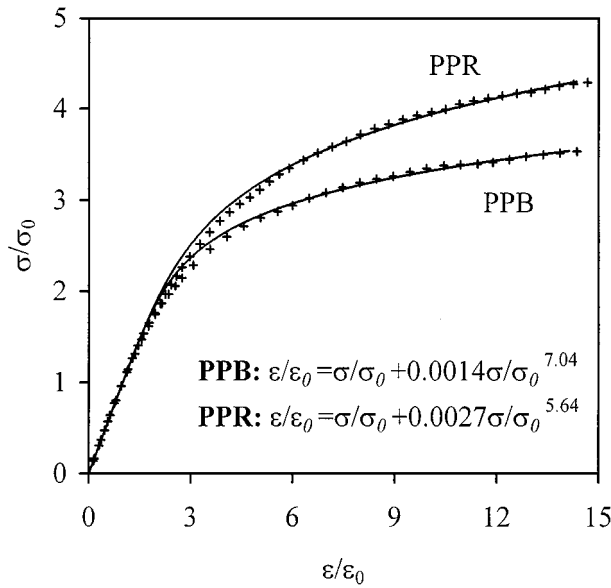


Figure 5 Stress/strain behaviour fitted to the Ramberg-Osgood equation. Symbols are the experimental data and line is the Ramberg-Osgood equation fit.

## 5. Application of normalization method

The extension of load separation principle to growing cracks was demonstrated by Sharobeam and Landes [8] with the condition that the crack growth starts beyond the non-separable region, i.e. once the plastic deformation pattern has been developed. In this work, once load separation validity was checked for both polypropylene copolymers, the load normalization method was applied in order to determine  $J$ - $R$  curves from a single fracture test. The resistance curves obtained have been analyzed according to variations applied in the method.

### 5.1. Determination of the deformation function, $H(v_{pl}/W)$

Firstly, normalized load was determined from fracture tests data and, it is worth noting that, in the case of the random copolymer ductile instability was observed, that is, unstable crack propagation occurred after a short stage of stable crack propagation. For this reason, fracture tests with PPR samples were stopped before the instability, being the final crack extension in this case lower than that developed in the fracture test on polypropylene block copolymer.

The deformation function was determined through the functional relationship between the normalized load and the normalized plastic displacement. As the crack length does not remain constant during loading of sharp-notched specimens, the main problem was to determine the range of  $P_N$  versus  $v_{pl}/W$  points where crack length was known and thus where these values could be correctly calculated. One point needed to determine  $H$  function is the final point of the test, which is obtained with the final values of load and displacement and with the crack length measured directly on the surface fracture of this specimen. The other points needed for  $H$  function belong to the early plastic deformation region in the  $P_N$  versus  $v_{pl}/W$  curve. For these points, an effective value of  $P_N$  and  $v_{pl}/W$  could be obtained

considering that no crack tip blunting occurred and that crack length remained thus constant.

In order to determine the limits of the region where load is separable and where crack length is constant, we employed the separation parameter,  $S_{pb}$ , as suggested by Cassanelli and De Vedia [26]. This parameter is defined as:

$$S_{pb} = \frac{P(a_p; v_{pl})}{P(a_b; v_{pl})} \Big|_{v_{pl}} \quad (15)$$

where p and b refer to pre-cracked and blunt notch specimen, respectively. The evolution of the separation parameter with plastic displacement is shown, for both copolymers, in Fig. 6. As long as crack remains stationary, the evolution of  $S_{pb}$  would be similar to that of  $S_{ij}$ , that is, after the non-separable initial region ( $v_{pl} > v_{plmin}$ ) the separation parameter would get a constant value. However, because of the crack tip blunting  $S_{pb}$  is not found totally constant but slightly decreases, and the value of plastic displacement where  $S_{pb}$  begins to be approximately constant ( $v_{plmin}$ ) defines the lower limit of the separable blunting region. This value results approximately the same that in the case of blunt notched specimens, that is,  $v_{plmin} \approx 0.2$  mm for PPB and  $v_{plmin} \approx 0.3$  for PPR. The crack growth initiation defines the upper limit of the separable blunting region because the slope of the  $S_{pb}$  versus  $v_{pl}$  plot changes from this point, decreasing more acutely the separation parameter value. Values of the upper limit of the separable blunting region were identified as  $v_{plmax} \approx 0.9$  mm for PPB and  $v_{plmax} \approx 0.7$  mm for PPR.

The evolution of  $P_N$  with the normalized plastic displacement ( $v_{pl}/W$ ) has been plotted in Fig. 7. Here, as mentioned before, despite the fact that crack tip

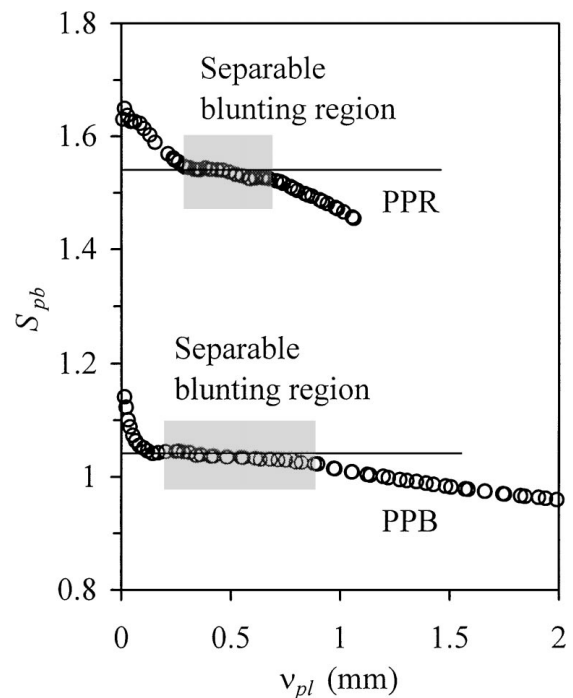


Figure 6 Evolution of the separation parameter  $S_{pb}$  with plastic displacement and determination of the limits of the separable blunting region.

blunting is experimentally observed and it can be analyzed through the separation parameter, its influence on the normalized load has been neglected as a first step of the normalization method application.

In Fig. 7, for  $H$  determination, a power law was employed to fit the normalized load values by using 6 points belonging to the separable blunting zone, and the final point. In order to give to this final point the same influence that to the initial points, it was set that the weight of the final point was six times higher than the weight of each point of the initial region. This fitting method is referred as “6 + 6” in opposition to the “6 + 1” method, which considers that the final point has the same weight that any of the initial points.

As it can be appreciated in Fig. 7b, the concordance found between the power law fit and the experimental data is poor for PPR sample, probably due to the short interval of stable crack propagation in this material. So, the power law fit utilization seems not to be very adequate for this grade of polypropylene when crack tip

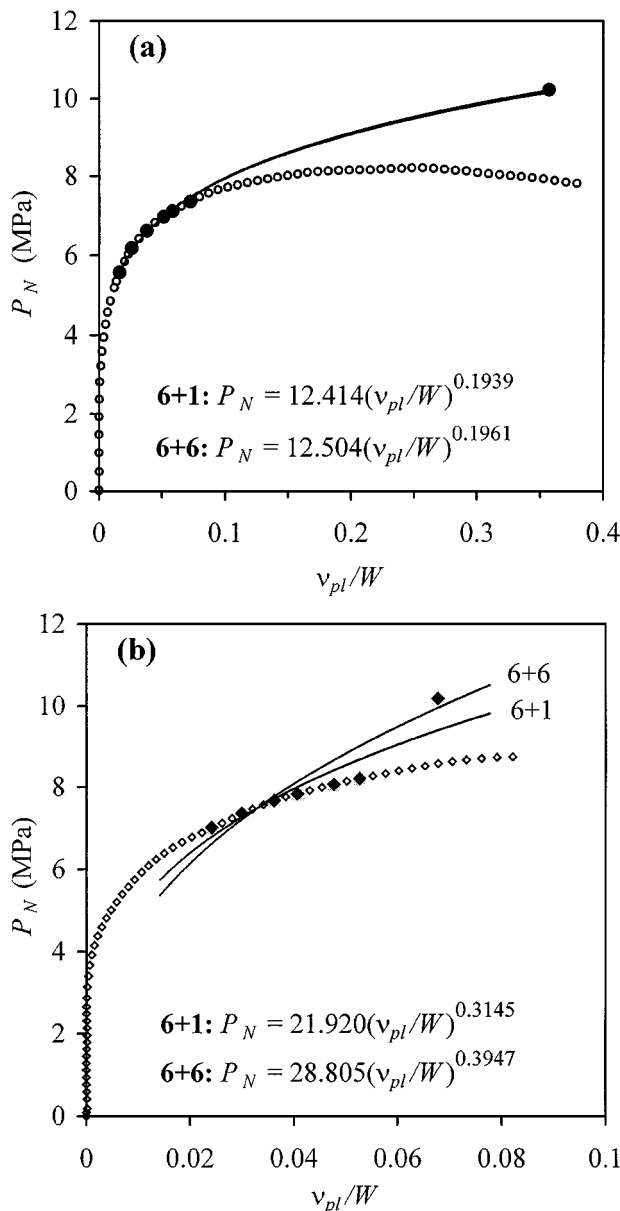


Figure 7 Determination of the deformation function for (a) PPB and (b) PPR specimens. Symbols were used for the power law fitting.

blunting is not taken into account. However, the concordance is found to be rather acceptable in PPB sample. Using the expressions of  $H(v_{pl}/W)$  obtained for this material, joint to the instantaneous values of  $P$  and  $d$ , the crack length could be calculated at each instant through Equations 11 and 14 by means of a numerical routine. So, once  $\Delta a$  was known, the  $J$ - $R$  curve of PPB could be easily plotted (Fig. 8a). Experimental points obtained by multiple specimen method [27] are also shown in this figure, for comparison.

Firstly, it can be observed that both “6 + 6” and “6 + 1” fitting methods resulted in  $J$ - $R$  curves almost identical for PPB polypropylene (Fig. 8a). For this polypropylene, independently of the weight that has been given to the final point, the  $J$ - $R$  curve determined from the normalization method shows more optimistic resistance to crack growth initiation than that obtained from multiple specimen data. In this sense,

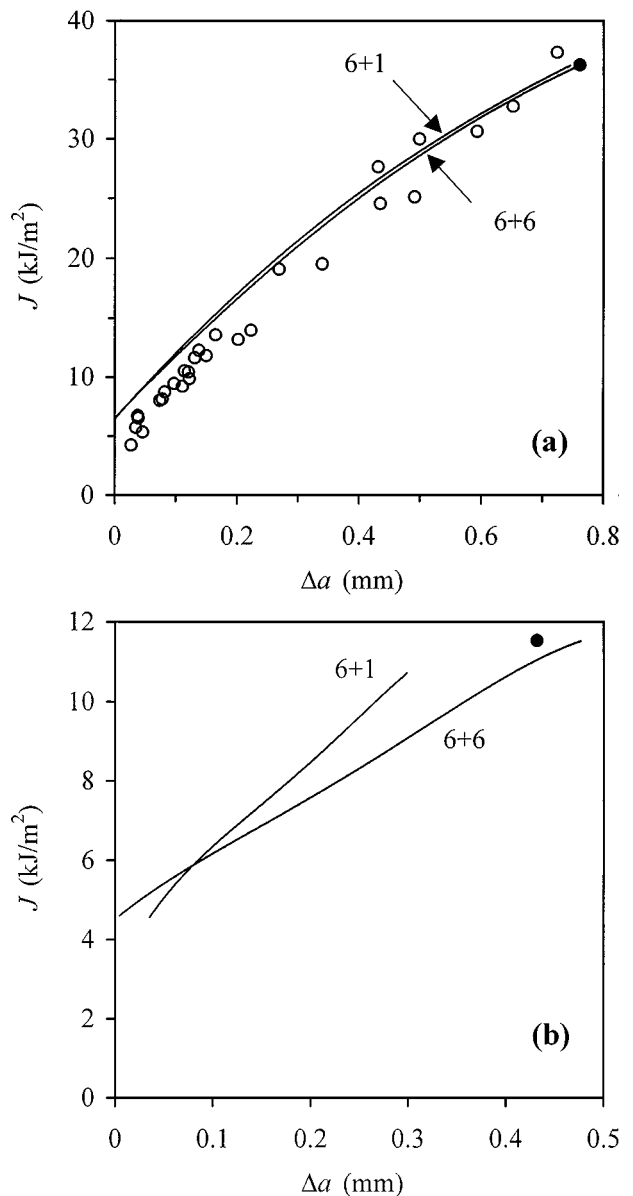


Figure 8  $J$ - $R$  curves obtained by the normalisation method for (a) PPB and (b) PPR using both 6 + 1 and 6 + 6 fitting methods. No crack tip blunting was taken into account. Symbols correspond to the points obtained from the multiple specimen method and the bold one corresponds to the particular specimen used for the normalisation method application.

not considering crack tip blunting introduces error in the normalization method application, since crack tip blunting is an important energy-consumption process that always occurs during crack propagation of ductile polymers. In following analysis, crack tip blunting will no longer be considered negligible.

On the other hand, due to the poor concordance found between the power law fit and the experimental  $P_N$  versus  $(v_{pl}/W)$  points for polypropylene random copolymer (PPR), the  $J$ - $R$  curve obtained from the normalization method have an important contribution of uncertainty. In this sense, as shown in Fig. 8b, the application of “6 + 6” and “6 + 1” fitting method resulted in  $J$ - $R$  curves very different. Moreover, due to its short range of stable crack propagation, it was not possible to obtain enough experimental points from multiple specimen fracture tests to plot a right resistance curve for this polypropylene, in order to use it as a reference.

## 5.2. Influence of crack tip blunting

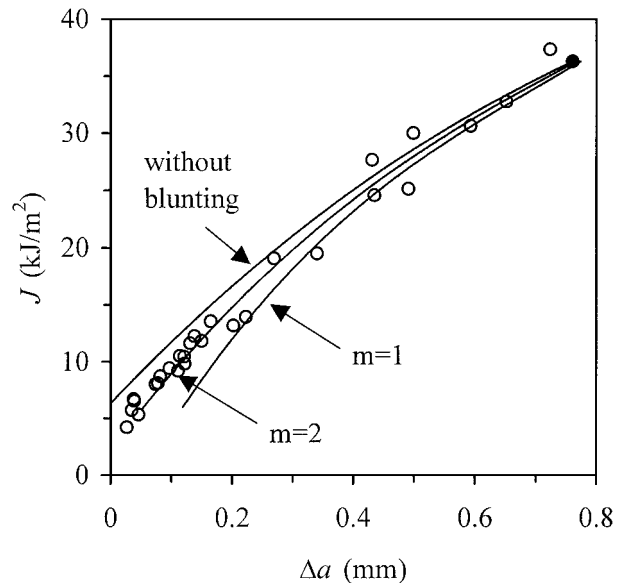
Here, crack tip blunting is considered for  $H(v_{pl}/W)$  determination by introducing an equivalent increment of crack extension ( $\Delta a_b$ ) through the blunting line general equation:

$$\Delta a_b = \frac{J_0}{2m\sigma_y} \quad (16)$$

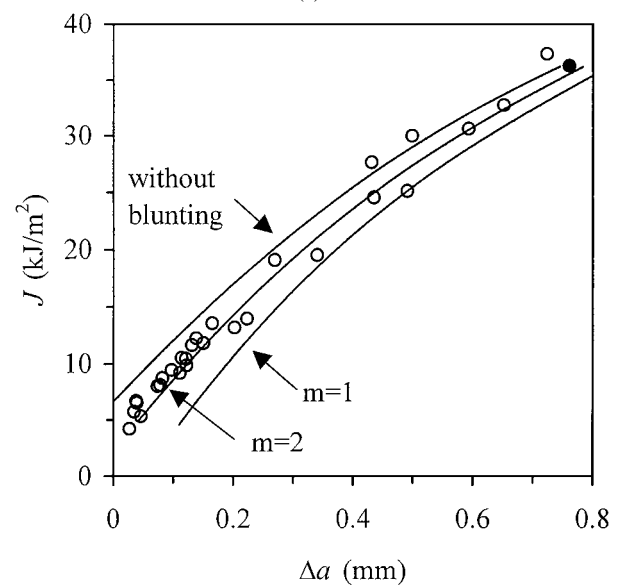
where  $m$  is the crack tip constraint factor and  $\sigma_y$  the material yield stress, which was adopted to be the maximum of the tensile stress/strain curve, determined at room temperature and at 1 mm/min on the injection-molded standard tensile specimens (Table I). The equivalent increment of crack extension was introduced in the calculus of both normalized load and plastic displacement.

Although a value of  $m = 1$  is usually accepted for Ramberg-Osgood materials, the constraint factor could be dependent on material (i.e. strengthening behavior), loading conditions (temperature, test speed...) and thickness and geometry of specimen (SENB, CT...). In this sense, Grellmann *et al.* report values of  $m = 0.7$  for a polypropylene homopolymer [28],  $m = 2$  for a PVC [13] and  $m = 0.5$ – $1$  for ABS with variable rubber content [29]. Due to this, although the stress/strain behavior of both copolymers of PP, shown in Fig. 5, seems to follow the Ramberg-Osgood equation, other values of the constraint factor (i.e.  $m = 2$ ) have been also used in this work in order to analyze its influence on the  $J$ - $R$  curves obtained from the normalization method, that is, to analyze how the crack tip blunting behavior affects the results of the normalization method application. In Fig. 9a the resulting  $J$ - $R$  curves obtained with different values of  $m$  are shown.

As mentioned before, if blunting is not considered an optimistic resistance curve results; however, the introduction of the blunting line general equation, as defined in ASTM standard [2] (i.e. with  $m = 1$ ) in  $H$  determination gives a more conservative  $J$ - $R$  curve, which is due to crack growth overestimation. This effect can be observed in Fig. 9a. When lower levels of crack tip blunting (higher values of  $m$ ) are considered in the analysis, a



(a)



(b)

Figure 9 Influence of the value of the crack tip constraint factor ( $m$ ) on the fracture resistance curves obtained for PP block copolymer using (a) the 6 + 6 and (b) the 6 + 1 power law fitting.

better concordance between results from both normalization and multiple specimen method is found. The best accuracy is found with a value of  $m$  close to 2 for PP block copolymer. In sight of this variation, it seems that the blunting line equation could be valid to introduce an equivalent increment of crack extension in the deformation function only when the material constraint factor is exactly known.

When blunting is considered in the analysis, the “6 + 6” fitting method seems to result more accurate than the “6 + 1” method, as it can be seen comparing Fig. 9a and b, because the first one promote the convergence of the resulting  $J$ - $R$  curve at higher level of crack growth, while the “6 + 1” method results in remarkable differences between the final value of  $\Delta a$  obtained by the normalization method and the experimental data. So, the fact of giving higher weight to the final point of the curve appears as a useful action in order to achieve better data convergence at the higher values of crack extension.



On the other hand, in order to analyze the influence of extension of the separable blunting region on the  $J$ - $R$  curve obtained from the normalization method, different separable blunting regions were considered. By one hand, "A" region was the separable blunting range determined using the separation parameter  $0.2 \text{ mm} < v_{pl} < 0.9 \text{ mm}$ . By the other hand, in order to minimize the influence of the crack tip blunting on  $H(v_{pl}/W)$  determination, two smaller separable blunting regions were considered and checked: "B" region ( $0.2 \text{ mm} < v_{pl} < 0.6 \text{ mm}$ ) and "C" region ( $0.2 \text{ mm} < v_{pl} < 0.3 \text{ mm}$ ). Fig. 10 shows the effect of these three separable blunting regions when they are considered separately in the normalization method, upon the resulting  $J$ - $R$  curve. In this figure, in order to maximize the influence of crack tip blunting,  $m$  was taken equal to 1. The coincidence between the  $J$ - $R$  curve obtained from this manner and that of the multiple specimen method at low values of  $\Delta a$  is better as the range of separable blunting is reduced. The explanation of this is the fact that the error associated to the use of the blunting line equation in the crack length values is reduced when smaller separable blunting regions are considered.

From the above analysis it results that  $J$ - $R$  curves with less uncertainty can be obtained using the first points of the separable blunting region ("C" zone) in the power law fitting, since the influence of the material crack tip blunting is so minimized, as it can be seen comparing Fig. 9a and Fig. 11.

### 5.3. Utilisation of the LMN function

Several authors [10, 13, 14] have found that the evolution of normalised load with plastic displacement can be better described by the LMN function than by the power law one. A general procedure for determining the three constants  $L$ ,  $M$  and  $N$  has been described in details by Landes *et al.* [10], being these constants

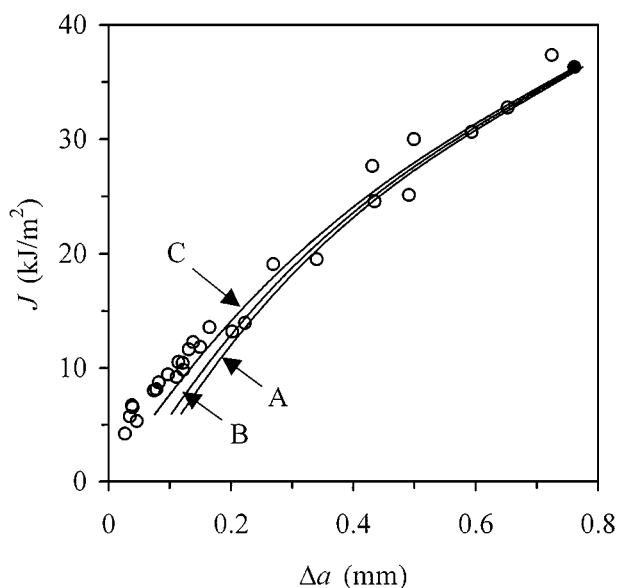


Figure 10 Influence of the separable blunting region extension on the  $J$ - $R$  curve using a power law fit. In these curves  $m$  was considered equal to 1 and a 6 + 6 fitting method was used.

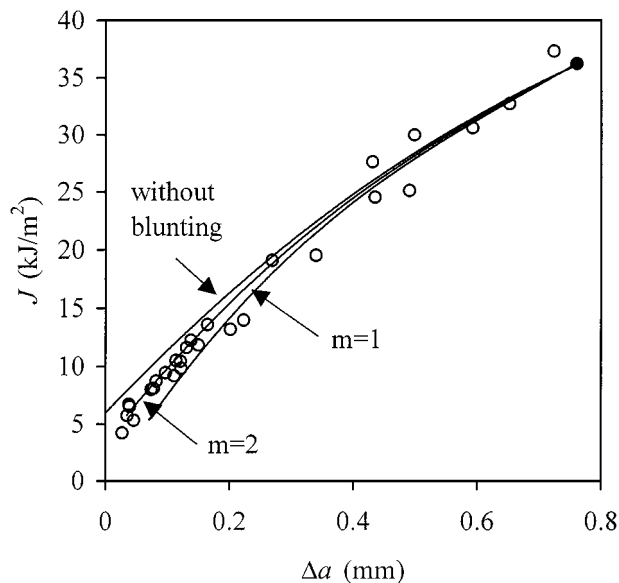


Figure 11 Influence of the value of the crack tip constraint factor ( $m$ ) on the fracture resistance curves obtained using a power law fit and region C.

determined through the use of three calibration points. Meanwhile the two first calibration points are the final point of the test and one point of the separable blunting region, as defined above for the power law fit, the third point has to be determined using a heavy iterative routine. Nevertheless, in the present work, a direct determination using a non-linear least squares fitting method from 6 points of the initial region of the curve and the final point was used, instead of the use of a third calibration point.

In Fig. 12, the application of both LMN and power law functions are shown comparatively for different values of  $m$ .

It can be noted that the LMN function coincides correctly with the final point of the curve without the necessity of giving a higher weight to this point, and also that both functions result almost equivalent in the separable blunting region because they describe a potential curve in this region. However, slight differences are observed between both fitting functions for values of plastic displacement close to the limit of the separable blunting region; particularly when crack tip blunting is not considered or it is over-estimated ( $m = 1$ ). Beyond crack growth initiation, the LMN function describes a straight line, which obviously differ from a potential trend. Nevertheless, both fitting functions coincide at the limit of the separable blunting region and also at the final point, since these points are part of the calibration points used to determine the constants of both functional forms.

The  $J$ - $R$  curves obtained using the LMN functions determined in Fig. 12 are shown in Fig. 13 for several crack tip-blunting behaviours.

Comparing these curves with those obtained from the power law (Fig. 9a), it can be noted that the use of different functional forms results in different trends of the  $J$ - $R$  curve. The best accuracy is found when  $m = 2$ . In this case, the  $J$ - $R$  curve obtained using the two fitting functions coincide at low and at high values of  $\Delta a$ , as it was observed for  $P_N$  in Fig. 12. Between these two

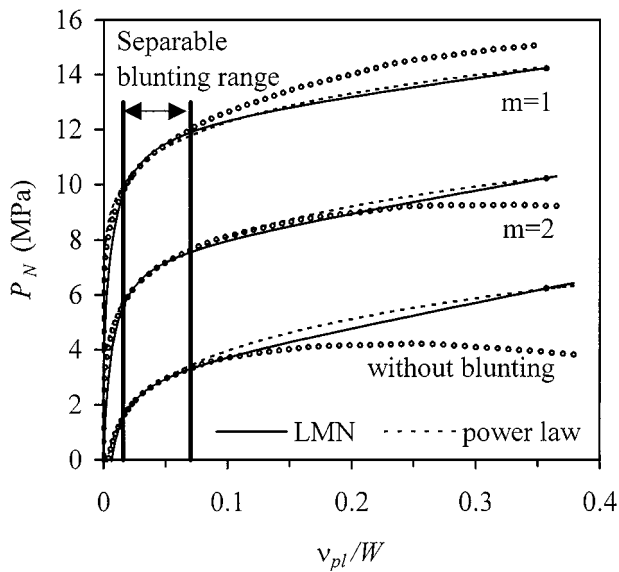


Figure 12 Comparison between the deformation function obtained using the power law and the LMN functional form. Different crack tip blunting behaviours are considered.

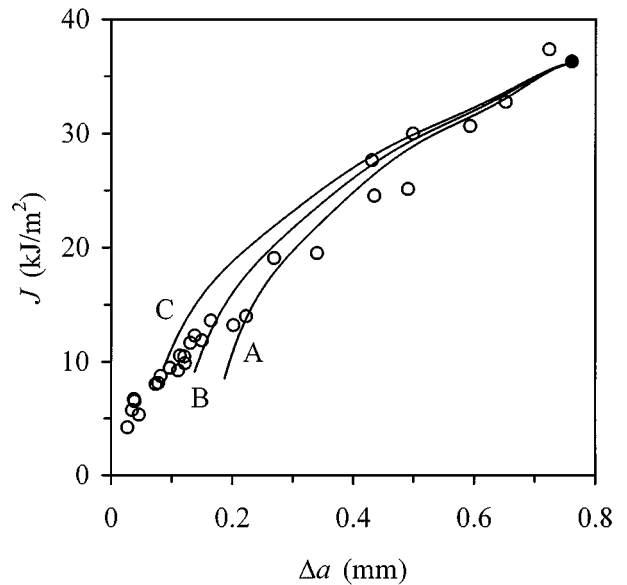


Figure 14 Influence of the separable blunting region extension on the  $J$ - $R$  curve using the LMN function. In these curves  $m$  was considered equal to 1.

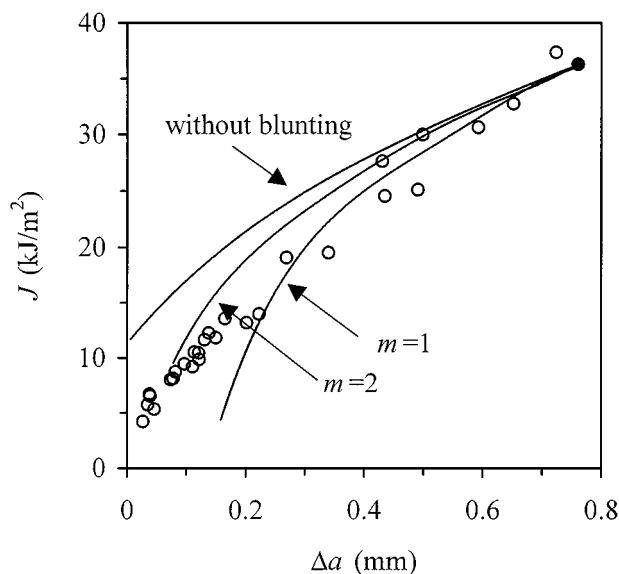


Figure 13 Influence of the value of the crack tip constraint factor ( $m$ ) on the fracture resistance curves obtained using the LMN function.

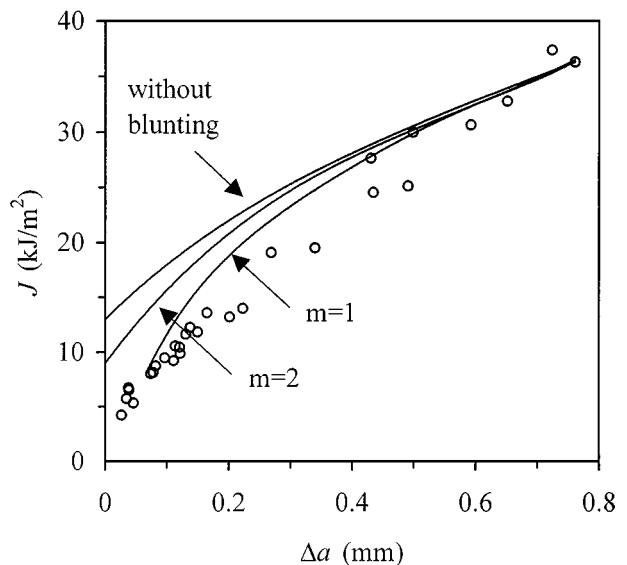


Figure 15 Influence of the value of the crack tip constraint factor ( $m$ ) on the fracture resistance curves obtained using the LMN function and region C.

regions, one can note that  $\Delta a$  is under-estimated by the use of the LMN function. This observation has to be associated with the fact that values of the normalised load predicted by the LMN function are, in this region, lower than those predicted by the power law. When others crack tip blunting behaviours are considered (no blunting and  $m = 1$ ), the differences observed in the initial part of the  $J$ - $R$  curve, respect to that of the multiple specimen data, are found higher than when the power law is used. The approximation introduced in the normalised load fitting has a notorious influence on the value of the crack length increment obtained by the numerical routine. For example, a difference of 0.22 MPa in the value of  $P_N$  predicted by the fitting functions involves a difference of 62  $\mu\text{m}$  in the value of  $\Delta a$ .

In a similar way than with the power law fitting the effect of several separable blunting ranges has been analysed with the LMN function, and the three resistance

curves obtained with the regions previously defined (A, B and C) are shown in Fig. 14, for a value of  $m = 1$ .

Again, the use of a shorter separable blunting range seems to result in a  $J$ - $R$  curve that is in good agreement with that of the multiple specimen method, particularly at low values of crack extension. Nevertheless, the differences between curves obtained from both methods are higher than using the power law fit in the normalisation method, as it can be noted comparing Fig. 14 and Fig. 10.

When different crack tip blunting behaviours are compared on the resultant  $J$ - $R$  curves obtained using region C (Fig. 15), the differences between them are found to be reduced in comparison with those observed in Fig. 13 for A region, since the influence of crack tip blunting is minimised when a shorter separable blunting range is considered. Nevertheless, this effect is not

very notorious and the differences are higher than when the power law was used (Fig. 11). For PPB sample with  $m = 2$  the use of C region results in lower concordance with results from the multiple specimen method than using A region (Fig. 11). This is due to the transition from a power law to a straight-line behaviour in the LMN function. If the separable blunting region is under-estimated (B and C regions), considerable error could be introduced in the deformation function, which would be transmitted to the  $J$ - $R$  resistance curve as underestimated  $\Delta a$  values. For this polymer, it could be concluded that the load normalisation method gives better results when the normalised load versus the plastic displacement is fitted using a power law equation. In this sense, Bernal *et al.* [23] also found better results for PP when a power law is used instead of the LMN function.

#### 5.4. Fracture parameters

From the above results, when the material crack tip blunting behaviour is not exactly known, a slightly conservative  $J$ - $R$  curve can be obtained using a power law fit calibrated with the very first points of the separable blunting region, and a value of  $m = 1$ . These conditions have been applied to both PP block and random copolymers and Fig. 16 presents the resulting  $J$ - $R$  curves.

The usually used  $J$ -integral critical values ( $J_{IC}$  and  $J_{0.2}$ ) have been determined following ASTM and ESIS recommendations from the resistance curves of Fig. 16. Also, a third critical value ( $J_{Spb}$ ) could be obtained from the energy at the maximum plastic displacement value ( $v_{plmax}$ ), considering this point as the crack propagation onset. Different critical values of  $J$ -integral have been obtained for PPB, considering several values of its crack tip constrain factor, using the power law or

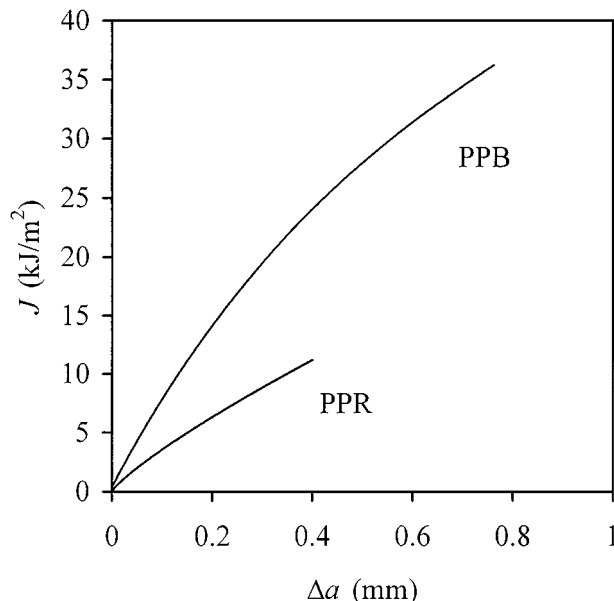


Figure 16  $J$ - $R$  curves obtained for both copolymers using the normalisation method with  $m = 1$  and a power law fit.

the LMN function, and employing different separable blunting regions. These values are compiled in Table III. The value of  $J_{Spb}$  is not affected by these variables.  $J$  critical values from the multiple specimen method are also shown for comparison.

Firstly, using a power law fit in the normalisation method and  $m = 2$ , the critical values of  $J$ -integral for PPB ( $14.6 < J_{0.2} < 15.2$  kJ/m<sup>2</sup>) are in good agreement with results from the multiple specimen method ( $J_{0.2} = 15.1$  kJ/m<sup>2</sup>) [27], independently of the separable blunting range considered. As pointed before on the resistance curves, considering no crack tip blunting results in a more optimistic  $J_{0.2}$  value, meanwhile

TABLE III Critical values of  $J$ -integral for PPB sample, determined through different methods and fitting function, and for different crack tip blunting behaviours. The several separable blunting ranges (A, B and C) were also used

Critical value of $J$ -integral (kJ/m <sup>2</sup> )	Normalisation Method using Power Law (6 + 6)								
	A			B			C		
	w.b.	$m = 1$	$m = 2$	w.b.	$m = 1$	$m = 2$	w.b.	$m = 1$	$m = 2$
$J_{IC}$	6.34	3.63	11.88	5.72	—*	12.14	5.78	—*	14.19
$J_{0.2}$	16.50	12.26	14.56	16.16	13.07	14.62	16.16	14.03	15.17
$J_{Spb}$					8.56				
Critical value of $J$ -integral (kJ/m <sup>2</sup> )	Normalisation Method using LMN (6 + 1)								
	A			B			C		
	w.b.	$m = 1$	$m = 2$	w.b.	$m = 1$	$m = 2$	w.b.	$m = 1$	$m = 2$
$J_{IC}$	11.17	3.77	22.71	11.45	2.35	23.76	12.81	—*	25.18
$J_{0.2}$	21.19	11.47	18.89	21.28	15.88	19.52	21.77	18.88	20.62
$J_{Spb}$					8.56				
Critical value of $J$ -integral (kJ/m <sup>2</sup> )	Multiple Specimen Method								
		w.b.			$m = 1$			$m = 2$	
$J_{IC}$		3.71			—*			14.7	
$J_{0.2}$					15.4				

\*  $J$ - $R$  curve and blunting line do not intersect.

introducing a crack blunting ( $m = 1$ ) gives a more conservative fracture resistance value. In this last case, the blunting line does not usually intersect with the  $J$ - $R$  curve, as it has been reported for polypropylene from resistance curves obtained with the multiple specimen method [30]. When A region is used, the over-estimation introduced in the crack length increment is so important that the resistance curve does intersect with the blunting line. Nevertheless, the corresponding critical value of  $J$ -integral results very low ( $J_{IC} = 3.6 \text{ kJ/m}^2$ ) for a material like polypropylene.

On the other hand, it is worth noting that the  $S_{pb}$  value ( $8.56 \text{ kJ/m}^2$ ) results more conservative than the critical values determined by the multiple specimen method. Theoretically,  $J_{IC}$  (for any  $m$  value) and  $J_{S_{pb}}$  should coincide, since the  $v_{plmax}$  is defined as the limit of the region where the crack length increment is only due to the crack tip blunting ( $\Delta a = \Delta a_b$ ), that is, the point where the resistance curve would diverge from the blunting line. Differences between  $J_{IC}$  and  $J_{S_{pb}}$  are due to the differences between the experimental values of normalised load and those of the power law fit.

Finally, for PPB the use of the LMN function in the normalisation method has resulted in over-estimated  $J$ -integral critical values, as it was expected from the more optimistic resistance curves obtained with this functional form.

## 6. Conclusions

The load separation validity has been studied for two polypropylene copolymers. After a short non-separable region, corresponding to the material elastic-plastic transition, the separation parameter gets a constant value over the plastic displacement, which confirms that load can be separated.

The normalisation method has been applied to determine the resistance curve, and several crack tip-blunting behaviours have been considered. Normalised load has been fitted either with a power law equation or with the so-called LMN function, and the resulting  $J$ - $R$  curves have been compared with those obtained by the multiple specimen method. It was shown that a correct resistance curve could be obtained using a power law fit to describe the evolution of normalised load with plastic displacement and that the material crack tip blunting has to be exactly known. For PP block copolymer, a high concordance between normalisation and multiple specimen methods was observed when a constraint factor  $m = 2$  was introduced in the blunting line equation.

The use of a reduced separable blunting region in the normalisation method minimised the influence of the material crack tip blunting on the resulting  $J$ - $R$  curve. This alternative was found to be a good solution when the polymer crack tip blunting behaviour is not exactly known.

Respect to the power law fit the use of the LMN function resulted in different trends of the  $J$ - $R$  curve. Beyond the separable blunting region, the crack length increment was under-estimated respect to the value

obtained by the multiple specimen method, and the  $J$ - $R$  curve was thus found to be more optimistic. Moreover, it was shown that using the LMN function, the influence of the crack tip blunting on the resistance curve was higher than when the power law was used. Nevertheless, in this case, the use of a shorter separable blunting region did not result in good accuracy.

## Acknowledgements

C. Morhain thanks the CIRIT (Generalitat de Catalunya, Spain) for the concession of a predoctoral grant.

## References

1. J. R. BEGLEY and J. D. LANDES, in "Fracture Toughness," STP 514 (ASTM, Philadelphia, 1972) p. 1.
2. ASTM E813-87 in "Annual Book of ASTM Standards," Part 10 (ASTM, Philadelphia, 1987) p. 686.
3. ESIS Technical Committee 4 (European Structural Integrity Society, March 1991).
4. J. R. LANDES and R. HERRERA, *Int. J. Fract.* **36** (1988) R9.
5. H. A. ERNST, P. C. PARIS, M. ROSSOW and J. W. HUTCHINSON, in "Fracture Mechanics," STP 677 (ASTM, Philadelphia, 1979) p. 581.
6. H. A. ERNST, P. C. PARIS and J. D. LANDES, in Fracture Mechanics: Thirteenth Conference, STP 743 (ASTM, Philadelphia, 1981) p. 476.
7. M. H. SHAROBEAM and J. D. LANDES, *Int. J. Fract.* **47** (1991) 81.
8. *Idem.*, *ibid.* **59** (1993) 213.
9. *Idem.*, *ibid.* **61** (1993) 379.
10. J. D. LANDES, Z. ZHOU, K. LEE and R. HERRERA, *J. Test. Eval.* **19** (1991) 305.
11. C. R. BERNAL, A. N. CASSANELLI and P. M. FRONTINI, *Polym. Test.* **14** (1995) 85.
12. C. R. BERNAL, P. E. MONTEMARTINI and P. M. FRONTINI, *J. Polym. Sci., Part B: Polym. Phys.* **34** (1996) 1869.
13. M. CHE, W. GRELLMANN, S. SEIDLER and J. D. LANDES, *Fatigue Fract. Engng. Mater. Struct.* **20** (1997) 119.
14. J. D. LANDES and Z. ZHOU, *Int. J. Fract.* **63** (1993) 383.
15. Z. ZHOU, J. D. LANDES and D. D. HUANG, *Polym. Engng. Sci.* **34** (1994) 128.
16. V. GARCIA-BROSA, C. BERNAL and P. FRONTINI, *Engng. Fract. Mech.* **62** (1999) 231.
17. R. HERRERA and J. D. LANDES, in Fracture Mechanics: Twenty-First Symposium, STP 1074 (ASTM, Philadelphia, 1990) p. 24.
18. T. W. ORANGE, in Fracture Mechanics: Twenty-First Symposium, STP 1074 (ASTM, Philadelphia, 1990) p. 545.
19. V. KUMAR, M. D. GERMAN and C. F. SHIH, An engineering approach for elastic-plastic fracture analysis, EPRI Report NP1931, 1981.
20. C. BERNAL, A. CASSANELLI and P. FRONTINI, *Polymer* **37** (1996) 4033.
21. J. R. RICE, *J. Appl. Mech.* **35** (1968) 379.
22. R. HERRERA and J. D. LANDES, *Int. J. Fract.* **16** (1988) 427.
23. C. BERNAL, M. RINK and P. FRONTINI, *Macromol. Symp.* **147** (1999) 235.
24. J. R. RICE, P. C. PARIS and J. G. MERKLE, in "Progress in Flaw Growth and Fracture Toughness Testing," STP 536 (ASTM, Philadelphia, 1973) p. 231.
25. J. CHAKRABARTY, "Theory of Plasticity" (McGraw-Hill, Singapore, 1987) p. 11.

26. A. N. CASSANELLI and L. A. DEVEDIA, *Int. J. Fract.* **83** (1997) 167.
27. J. I. VELASCO, C. MORHAIN, D. ARENCÓN, O. O. SANTANA and M. L. MASPOCH, *Polymer Bulletin* **41** (1998) 615.
28. W. GRELLMANN and M. CHE, *J. Appl. Polym. Sci.*, **66** (1997) 1237.
29. Y. HAN, R. LACH and W. GRELLMANN, *Angew. Makromol. Chemie* **270** (1999) 13.
30. I. NARISAWA, *Polym. Engng. Sci.* **271**(1) (1987) 41.

*Received 30 July 1999  
and accepted 14 August 2000*